

Transport properties of protic ionic liquids, pure and in aqueous solutions: Effects of the anion and cation structure

Anouti, M., Jacquemin, J., & Lemordant, D. (2010). Transport properties of protic ionic liquids, pure and in aqueous solutions: Effects of the anion and cation structure. *Fluid Phase Equilibria*, 297(1), 13-22. DOI: 10.1016/j.fluid.2010.05.019

Published in:
Fluid Phase Equilibria

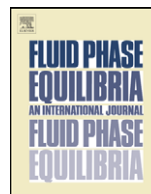
Queen's University Belfast - Research Portal:
[Link to publication record in Queen's University Belfast Research Portal](#)

General rights

Copyright for the publications made accessible via the Queen's University Belfast Research Portal is retained by the author(s) and / or other copyright owners and it is a condition of accessing these publications that users recognise and abide by the legal requirements associated with these rights.

Take down policy

The Research Portal is Queen's institutional repository that provides access to Queen's research output. Every effort has been made to ensure that content in the Research Portal does not infringe any person's rights, or applicable UK laws. If you discover content in the Research Portal that you believe breaches copyright or violates any law, please contact openaccess@qub.ac.uk.



Transport properties of protic ionic liquids, pure and in aqueous solutions: Effects of the anion and cation structure

Meriem Anouti*, Johan Jacquemin, Daniel Lemordant

Université François Rabelais, laboratoire PCMB (EA 4244), équipe Chimie-physique des Interfaces et des Milieux Electrolytiques (CIME), Parc de Grandmont, 37200 Tours, France

ARTICLE INFO

Article history:

Received 8 December 2009
Received in revised form 17 May 2010
Accepted 21 May 2010
Available online 27 May 2010

Keywords:

Protic ionic liquids
Ionic conductivity
Molar conductivity
Self-diffusion coefficient
Hydrodynamic radius

ABSTRACT

Ionic conductivities of twelve protic ionic liquids (PILs) and their mixtures with water over the whole composition range are reported at 298.15 K and atmospheric pressure. The selected PILs are the pyrrolidinium-based PILs containing nitrate, acetate or formate anions; the formate-based PILs containing diisopropylethylammonium, amilaminium, quinolinium, lutidinium or collidinium cations; and the pyrrolidinium alkylcarboxylates, [Pyrr][C_nH_{2n+1}COO] with $n = 5-8$. This study was performed in order to investigate the influence of molecular structures of the ions on the ionic conductivities in aqueous solutions. The ionic conductivities of the aqueous solutions are 2–30 times higher than the conductivities of pure PILs. The maximum in conductivity varies from $w_w = 0.41$ to 0.74 and is related to the nature of cations and anions. The molar conductance and the molar conductance at infinite dilution for (PIL + water) solutions are then determined. Self-diffusion coefficients of the twelve protic ionic liquids in water at infinite dilution and at 298.15 K are calculated by using the Nernst–Haskell, the original and the modified Wilke–Chang equations. These calculations show that similar values are obtained using the modified Wilke–Chang and the Nernst–Haskell equations. Finally, the effective hydrodynamic (or Stokes) radius of the PILs was determined by using the Stokes–Einstein equation. A linear relationship was established in order to predict this radius as a function of the anion alkyl chain length in the case of the pyrrolidinium alkylcarboxylates PILs.

© 2010 Elsevier B.V. All rights reserved.

1. Introduction

The term ionic liquid (IL) is broadly used in order to describe a large class of low melting organic molten salts liquids below 100 °C. Protic ionic liquids (PILs) are a subset of ionic liquids formed by the stoichiometric (equimolar) combination of a Brønsted acid with a Brønsted base [1–4]. When a PIL is synthesised by mixing a strong acid with a strong base, the proton is located very strongly on the base; the PIL is most likely composed entirely of ions with possible ion complexation and aggregate formation [5].

ILs have received a great attention as a class of solvents with a wide range of potential applications including organic and inorganic synthesis [6], energy storage devices [7], separations [8,9], and catalysis [10]. The most notable characteristics of many ionic liquids are their low vapour pressure, non-flammability, thermal stability, wide liquid range, and solvating properties for diverse substances. PILs are characterized by their great ability to form H-bond and present by consequence a strong interaction with polar solvents. For this reason, they have been investigated as amphiphile

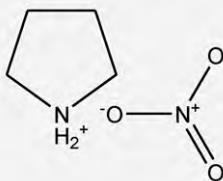
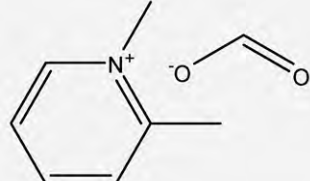
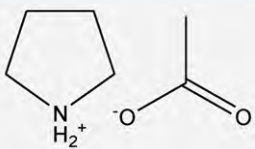
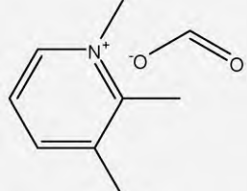
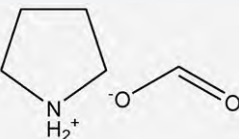
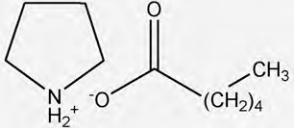
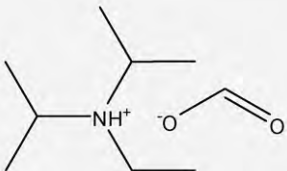
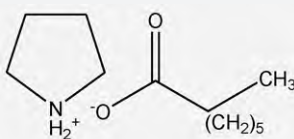
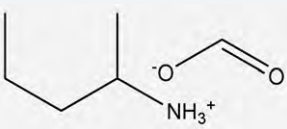
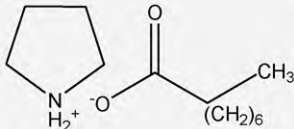
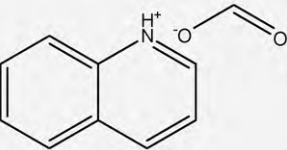
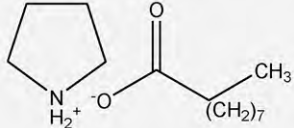
self-assembly media [11], biological solvents [12], and in polymer membrane fuel cells [13].

Among the most important properties of ionic liquids is their conductivity for potential application as electrolytes in electrochemical devices. PILs can be mixed with water and protic solvents, consequently, provide new opportunities for studying the conductivity of electrolyte solutions in salt-rich region. There are a number of studies concerning the specific conductivity and viscosities of pure aprotic ILs (IL + molecular solvent) mixtures and (IL + polymer) composites [14–23]. It is desirable and of great importance to understand and predict the transport properties of (IL + molecular solvent) solutions by mean of theoretical models.

In this work, we present experimental measurements of ionic conductivities of twelve protic ionic liquids and their mixtures with water over the whole composition range at 298.15 K and atmospheric pressure. The molar conductivities at infinite dilution of the selected PILs are determined by fitting the experimental data of ionic conductivities of (PIL + water) systems. From these results, the infinite dilution conductances of cations and anions of investigated PILs were then obtained. The self-diffusion coefficients were also calculated by using original/modified Wilke–Chang and the Nernst–Haskell equations. These diffusion coefficient calculations using both of these equations are convergent. Finally, the effective

* Corresponding author. Tel.: +33 247366951; fax: +33 247367360.
E-mail address: meriem.anouti@univ-tours.fr (M. Anouti).

Table 1
Name, abbreviation and structure of studied PILs.

Protic ionic liquid name, abbreviation	Structure	Protic ionic liquid name, abbreviation	Structure
Pyrrolidinium nitrate [Pyrr][NO ₃] (1)		Lutidinium formate [Luti][HCOO] (7)	
Pyrrolidinium acetate [Pyrr][CH ₃ COO] (2)		Collidinium formate [Coll][HCOO] (8)	
Pyrrolidinium formate [Pyrr][HCOO] (3)		Pyrrolidinium hexanoate [Pyrr][C ₅ H ₁₁ COO] (9)	
Diisopropylethylammonium formate [DIPEA][HCOO] (4)		Pyrrolidinium heptanoate [Pyrr][C ₆ H ₁₃ COO] (10)	
Amilaminium formate [Amil][HCOO] (5)		Pyrrolidinium octanoate [Pyrr][C ₇ H ₁₅ COO] (11)	
Quinolinium formate [Qui][HCOO] (6)		Pyrrolidinium nonanoate [Pyrr][C ₈ H ₁₇ COO] (12)	

hydrodynamic (or Stokes) radius of PILs was determined through the Stokes–Einstein equation.

2. Experimental

2.1. Materials

All amines (pyrrolidine, diisopropylamine, collidine, amilamine, and quinoline), and organic acids (formic, acetic, pentanoic, hexanoic, heptanoic, and octanoic acids) are commercially available from Fluka (>99.0%) and are used without further purification. The nitric acid (68% in water) solution is obtained from Sigma–Aldrich. Water is purified with Milli-Q 18.3 MΩ water system and 1,2-dichloroethane DCE (>99.0%) is purchased from Sigma–Aldrich.

2.2. Preparation of PILs

Pyrrolidinium-based PILs (1–3) containing [NO₃][−], [CH₃COO][−], or [HCOO][−], anions and diisopropylethylammonium formate (4)

are synthesised and purified following the procedure described in detail in previous works [24,25] and summarized below. The preparation of four new PILs, based on the formate anion and different cations: amilaminium (5), quinolinium (6), lutidinium (7) and collidinium (8) are obtained by neutralization of corresponding amines by the formic acid. The pyrrolidinium alkylcarboxylates ([Pyrr][C_nH_{2n+1}COO] with *n* = 5–8) (9–12), which exhibit a higher ability to aggregate in aqueous solution forming a novel class of anionic surfactants, are prepared through the neutralization of pyrrolidine by alkylcarboxylic acids according to the procedure described in a previous work [26].

For the preparation of [Pyrr][NO₃] (1), pyrrolidine (26.78 g; 0.37 mol) is introduced in a two-necked round-bottom flask immersed in an ice bath. Nitric acid (68% in water) (34.54 g; 0.37 mol) is added dropwise to the flask in about 60 min. To get rid of residual water, 120 mL of DCE is added and azeotropic (DCE+water) mixture is distilled. DCE is finally evaporated from the mixture under reduced pressure so that

Table 2Properties of studied PILs: molar mass (M), density (ρ), molar volume (V_m), viscosity (η), specific (σ) and molar ionic conductivity (Λ), and their uncertainty at 298.15 K.

PILs (water content in ppm)	M (g mol ⁻¹)	ρ (g cm ⁻³) $\pm 0.1\%$	V_m (cm ³ mol ⁻¹) $\pm 0.1\%$	η (mPa s) $\pm 0.1\%$	σ (mS cm ⁻¹) $\pm 2\%$	Λ (S cm ² mol ⁻¹) $\pm 2\%$
[Pyr][NO ₃] (1) (300)	134.13	1.1676	114.88	5.2	50.12	5.75
[Pyr][CH ₃ COO] (2) (500)	131.20	1.0543	124.44	30.2	5.94	0.73
[Pyr][HCOO] (3) (100)	117.08	1.1190	104.63	2.5	32.95	3.44
[DIPEA][HCOO] (4) (50–80)	175.16	1.0144	172.68	18.0	5.80	0.86
[Amil][HCOO] (5) (20–35)	133.15	1.1630	114.49	nd	0.35	0.04
[Qui][HCOO] (6) (170)	175.19	1.1530	151.94	8.20	4.15	0.63
[Luti][HCOO] (7) (80–90)	167.20	1.0209	163.77	2.61	10.40	1.70
[Coll][HCOO] (8) (100)	153.18	1.1676	148.72	10.0	6.71	1.11
[Pyr][C ₅ H ₁₁ COO] (9) (30)	187.28	0.9880	189.43	27.4	1.95	0.31
[Pyr][C ₆ H ₁₃ COO] (10) (45–60)	201.31	0.9721	207.09	nd	1.02	0.21
[Pyr][C ₇ H ₁₅ COO] (11) (80)	215.30	0.9495	226.99	36.5	0.81	0.18
[Pyr][C ₈ H ₁₇ COO] (12) (120)	229.36	0.9315	246.05	74.4	0.63	0.15

a pale yellow and viscous liquid can be collected (yield: 93%).

Only the preparation of [Pyr][HCOO] is reported in this work as a similar procedure applied for other compounds (2–11). Pyrrolidine (38.55 g; 0.85 mol) is placed in a three-neck round-bottom flask immersed in an ice bath and equipped with a reflux condenser, formic acid (61.45 g; 0.85 mol) is added to the pyrrolidine under vigorous stirring (60 min). The residual amine or acid is evaporated under reduced pressure at 353 K to obtain the target PIL (98.72 g; yield: 98.7%).

All synthesised PILs were dried overnight at 343 K under high vacuum (1 Pa) prior to use. Ionic liquids were analysed for water content using a coulometric Karl–Fischer titration prior any measurements. The water content of the PILs, measured just after distillation, is in range of 20–50 ppm, depending on the nature of PILs. The purity of PILs was checked by ¹H NMR spectrum using a 200 MHz Bruker spectrometer, CDCl₃ as solvent and TMS as internal standard. Obtained PILs are also characterized by differential scanning calorimetry (DSC), pycnometry, and rheology.

2.3. Measurements

Viscosities are measured using a TA instrument rheometer (AR 1000) with cone-plan geometry at various temperatures (from 298 to 353 K), values are given with accuracy greater than $\pm 0.1\%$. Differential scanning calorimetry (DSC) is carried out on a Perkin Elmer DSC6 under N₂ atmosphere. The densities of protic ionic liquid were measured using a Sartorius 1602 MP balance with an accuracy of $\pm 10^{-4}$ g and pycnometers immersed in a thermostated bath. The densities values for water as reference, is ρ (g cm⁻³) = 0.9971 at 298 K. The uncertainty for densities did not exceed $\pm 0.1\%$. Conductivity measurements were performed by using a Crison (GLP 31) digital multi-frequencies conductimeter, between 1000 and 5000 Hz. The temperature control (at $T = 298.15 \pm 0.02$ K) is ensured by a JULABO thermostated bath. The conductimeter was calibrated with standard solutions of known conductivity (0.1 and 0.02 mol L⁻¹, KCl), the uncertainty for conductivities did not exceed $\pm 2\%$. The conductivity measurements of the PILs in aqueous solutions were carried out by continuous addition of pure PILs into water. Each conductivity was recorded when its stability was better than 1% within 2 min.

The names, and chemical formula of investigated compounds, are represented in Table 1.

3. Results and discussion

3.1. Physical properties of pure PILs

Physicochemical characteristics: molar mass, density, molar volume, viscosity, specific and molar ionic conductivity of PILs at 298.15 K and their uncertainty are listed in Table 2. The uncer-

tainties for ρ , η and σ are deduced from measurements, whereas for V_m , and Λ , uncertainties are obtained from the computed values.

Ionic liquid densities are typically in the range 0.9–1.6 g cm⁻³ [11]. Generally, the ILs density is very strongly affected by the nature of the anion. For the studied PILs, densities fall in the range 1.1676–0.9690 g cm⁻³ as shown in Table 2, and are related to the compactness of their structures. In fact the density decreases for pyrrolidinium with alkylcarboxylates as counter anion [Pyr][C_nH_{2n+1}COO] series when the alkyl chain length increases: $\rho = 1.0246$ g cm⁻³ ($n = 5$); 1.0037 g cm⁻³ ($n = 6$), 0.9870 g cm⁻³ ($n = 7$), 0.9690 g cm⁻³ ($n = 8$). We note also that pyrrolidinium nitrate posses the higher density $\rho = 1.1676$ g cm⁻³ and lower molar volume deduced from its structure.

The nature of the anion and the cation, which compose the ionic liquid, has a huge effect on their viscosity. PILs viscosities studied in this works are reported in Table 2. As already described in previous work [26], the relative significance of van der Waals interactions increases with a long alkyl chain length, for [Pyr][C_nH_{2n+1}COO] series and their viscosities vary from 27.4 to 74.4 cP (with 1 cP = 1 mPa s). Viscosity increases also with a high degree of branching of anion $\eta = 2.5$ cP for [Pyr][HCOO] and $\eta = 30.2$ cP for [Pyr][CH₃COO], respectively; or high degree of branching of cation $\eta = 2.6$ cP for [Luti][HCOO] and $\eta = 10.0$ cP for [Coll][HCOO], respectively.

At 298.15 K, the conductivity values of PILs are from 0.35 to 50.12 mS cm⁻¹ (Table 2). It appears that, both natures of anions and cations impact conductivity values. This transport property is correlated to the viscosity of medium and ions mobility. The

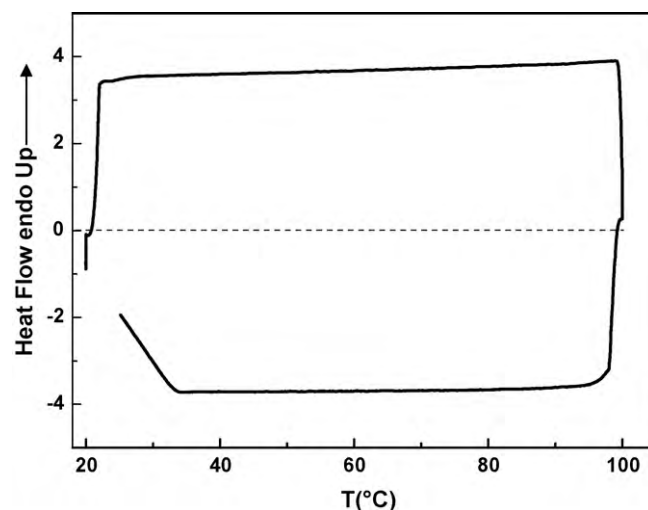


Fig. 1. DSC thermogram of pyrrolidinium octanoate, [Pyr][C₇H₁₅COO].

Table 3
Conductivities, σ , for the binary mixtures of (PIL + water) as a function of water weight fraction percentage, w_w , at 298.15 K.

w_w (%)	σ (mS cm ⁻¹)	w_w (%)	σ (mS cm ⁻¹)	w_w (%)	σ (mS cm ⁻¹)	w_w (%)	σ (mS cm ⁻¹)
[Pyrr][NO₃] (1)		[Pyrr][CH₃COO] (2)		[Pyrr][HCOO] (3)		[DIPEA][HCOO] (4)	
0.00	50.10	0.00	5.94	0.00	32.9	0.00	5.86
4.76	67.90	4.74	6.85	2.51	40.06	6.25	8.80
9.08	77.40	9.06	7.16	5.01	44.42	11.76	11.33
16.65	91.10	16.61	10.38	9.07	49.5	16.67	13.92
19.99	97.00	19.94	11.08	16.66	59.9	21.05	16.65
25.91	104.10	25.85	15.28	23.04	67.1	25.00	19.55
31.01	108.60	30.95	19.28	28.53	72	31.82	24.00
35.46	110.50	35.39	23.18	33.29	75.4	34.78	26.30
39.37	113.30	39.30	26.38	37.45	77.3	42.31	31.10
45.92	111.90	45.85	32.38	41.13	78.3	46.43	33.60
49.98	108.30	49.90	35.18	44.39	78.3	50.00	35.10
55.53	109.50	55.46	39.18	49.95	77.7	55.88	38.60
59.98	104.30	59.90	40.88	56.47	73.3	58.33	39.30
65.50	99.70	65.43	42.98	58.28	70.4	60.53	39.60
70.13	94.20	70.07	43.68	66.62	63.6	62.50	39.70
79.99	78.60	75.54	44.28	70.55	59.2	64.29	39.70
85.04	61.00	80.33	42.28	74.96	53.6	65.91	39.60
90.74	45.00	83.28	40.18	79.97	44.8	70.00	39.70
96.00	25.00	100.00	0.001	86.07	31.8	71.15	39.70
99.87	1.22			90.18	21.3	72.22	39.60
100.00	0.001			91.06	18.8	100.00	0.001
				100.00	0.001		
w_w (%)	σ (mS cm ⁻¹)	w_w (%)	σ (mS cm ⁻¹)	w_w (%)	σ (mS cm ⁻¹)	w_w (%)	σ (mS cm ⁻¹)
[Amil][HCOO] (5)		[Qui][HCOO] (6)		[Luti][HCOO] (7)		[Coll][HCOO] (8)	
0.00	0.36	0.00	4.15	0.00	10.40	0.00	6.80
5.60	1.21	5.66	6.21	5.10	13.74	4.76	8.37
10.05	1.97	9.09	8.54	9.08	16.39	9.09	9.63
16.23	3.42	16.67	13.76	16.65	22.10	16.66	13.30
27.93	8.47	20.00	15.94	28.54	32.70	19.99	14.80
36.76	13.75	25.93	20.10	33.30	37.70	25.92	18.81
43.66	19.23	31.03	24.70	41.14	45.20	31.03	23.10
53.75	28.00	35.48	28.40	44.41	47.40	35.47	26.90
60.78	33.00	39.39	31.00	49.97	52.60	41.17	32.30
65.95	35.10	44.44	34.90	54.51	55.56	45.94	36.20
69.92	36.00	45.95	35.90	61.51	59.80	49.99	39.50
75.61	35.70	50.00	38.10	65.49	61.60	55.55	43.70
79.99	34.00	56.52	41.10	70.56	62.30	59.99	46.50
88.00	29.30	60.00	42.30	76.17	60.00	65.51	47.40
90.00	27.30	65.52	43.00	79.98	56.80	70.14	47.50
91.00	23.80	70.59	42.60	85.70	48.50	74.99	47.50
92.50	21.30	75.00	41.20	87.48	45.10	79.99	45.10
93.30	19.36	80.00	39.40	88.88	42.10	85.71	38.50
94.30	17.11	85.71	33.70	89.99	39.30	90.00	31.30
95.40	14.65	90.00	27.50	90.90	37.00	95.00	19.31
96.70	11.29	100.00	0.001	100.00	0.001	100.00	0.001
98.20	6.77						
100.00	0.001						
w_w (%)	σ (mS cm ⁻¹)	w_w (%)	σ (mS cm ⁻¹)	w_w (%)	σ (mS cm ⁻¹)	w_w (%)	σ (mS cm ⁻¹)
[Pyrr][C₅H₁₁COO] (9)		[Pyrr][C₆H₁₃COO] (10)		[Pyrr][C₇H₁₅COO] (11)		[Pyrr][C₈H₁₇COO] (12)	
0.00	2.04	0.00	1.86	0.00	0.80	0.00	0.64
4.76	5.68	4.76	5.28	4.75	2.23	4.76	0.73
9.09	9.50	9.09	7.40	9.08	3.47	9.09	1.22
14.89	15.44	14.89	11.28	16.64	6.35	16.67	2.95
16.67	17.33	20.00	14.13	19.97	7.95	20.00	3.92
18.37	19.14	25.93	18.00	25.89	10.64	25.93	5.79
20.00	20.10	28.57	19.68	31.00	13.10	31.03	7.54
23.08	22.10	31.03	21.19	35.44	15.85	35.48	9.15
25.93	24.00	33.33	22.22	39.35	17.04	39.39	10.72
27.27	24.80	35.48	23.09	45.90	19.25	45.95	12.90
29.82	26.10	37.50	23.83	49.96	20.60	50.00	14.35
31.03	26.50	39.39	24.17	55.51	21.80	55.56	16.14
33.33	27.60	40.30	24.39	59.96	22.30	58.33	16.83
35.48	28.60	42.03	24.70	62.92	22.30	60.00	17.32
38.46	29.10	44.44	25.26	65.48	22.20	61.54	17.64
40.30	29.10	45.95	25.57	70.11	21.70	62.96	17.89
45.21	29.20	48.72	25.91	75.58	20.30	64.29	18.13
50.00	28.90	50.00	26.00	77.24	19.66	65.52	18.37
52.94	28.50	52.38	26.13	80.37	18.26	66.67	18.46
55.06	28.10	55.56	26.17	82.12	16.76	71.43	18.70
60.10	25.31	60.8	24.67	100.00	0.001	80.65	16.31
70.15	19.64	70.11	21.21			90.20	10.83
80.04	12.11	80.50	15.16			100.00	0.001
90.02	5.51	90.50	7.28				
100.00	0.001	100.00	0.001				

Table 4

Obtained parameters from conductivity measurements for studied PILs in aqueous solution at 298.15 K.

PILs	σ_{\max} (mS cm ⁻¹)	$w_{w(\max)}$ (%)	Λ^0 (PILs) (S cm ² mol ⁻¹)	Λ^0 (cation) (S cm ² mol ⁻¹)	Λ^0 (anion) (S cm ² mol ⁻¹)
[Pyrr][NO ₃] (1)	113.0	41.15	130.4	60.0	74.4
[Pyrr][CH ₃ COO] (2)	44.5	74.27	101.1	60.0	40.9
[Pyrr][HCOO] (3)	78.3	41.13	114.6	60.0	54.6
[DIPEA][HCOO] (4)	39.7	64.28	84.6	30.0	54.6
[Amil][HCOO] (5)	36.0	69.90	65.1	10.1	54.6
[Qui][HCOO] (6)	43.0	65.50	68.6	14.0	54.6
[Luti][HCOO] (7)	62.3	70.50	100.2	45.6	54.6
[Coll][HCOO] (8)	47.6	58.70	90.2	35.6	54.6
[Pyrr][C ₅ H ₁₁ COO] (9)	29.2	43.00	87.2	60.0	27.2 ^a
[Pyrr][C ₆ H ₁₃ COO] (10)	26.7	55.50	85.3	60.0	25.2 ^a
[Pyrr][C ₇ H ₁₅ COO] (11)	22.0	62.20	84.0	60.0	23.1 ^a
[Pyrr][C ₈ H ₁₇ COO] (12)	18.0	71.40	83.0	60.0	22.7 ^a

Conductivities (σ_{\max}) and weight fraction of water ($w_{w(\max)}$) at maximum; molar conductivities of ionic liquids (Λ^0 (PILs)), cation (Λ^0 (cation)) and anion (Λ^0 (anion)) at infinite dilution.

^a Limit molar conductivities Λ^0 (anion) from the literature [34].

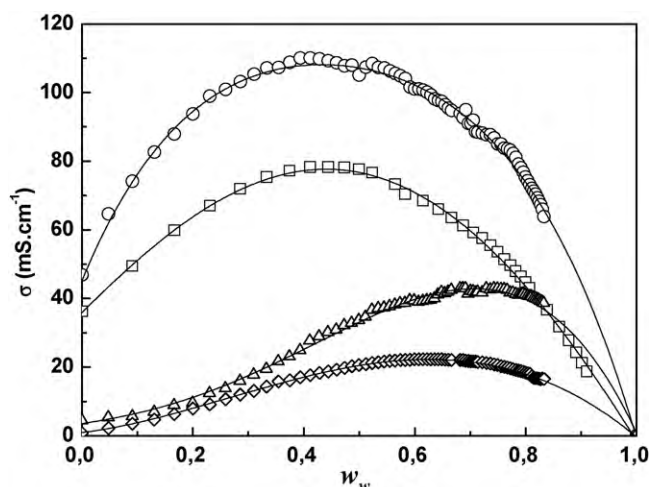


Fig. 2. Ionic conductivity, σ , versus the water weight fraction, w_w , in the aqueous PILs mixtures for pyrrolidinium-based PILs: \circ , [Pyrr][NO₃] (1); Δ , [Pyrr][CH₃COO] (2); \square , [Pyrr][HCOO] (3); \diamond , [Pyrr][C₇H₁₅COO] (11).

conductivity values of [Pyrr][NO₃] and [Pyrr][HCOO], $\sigma = 50.12$ and 32.95 mS cm⁻¹, respectively, are higher than other studied PILs because these PILs are good or superionic liquids according to Walden classification rule [25].

The thermal behaviour of the twelve studied PILs was investigated by differential scanning calorimetry (DSC). Each studied PILs exhibit a similar thermogram over ambient temperature. In Fig. 1, we have shown for example the thermogram for the pyrrolidinium octanoate, it is a typical thermogram observed for all investigated PILs into this study. We observe in Fig. 1 that [Pyrr][C₇H₁₅COO] does not present any transition peak from 293 to 373 K, it is the case of all studied PILs.

3.2. Physical properties of (PIL + water) binary systems

The ionic conductivity values, for (PIL + water) binary systems, were measured at 298.15 K, as function of the water weight fraction, w_w . The data for specific conductivity, σ , for the studied solutions are presented in Table 3. In Table 4 are reported the maximum of conductivities (σ_{\max}) and water weight fraction ($w_{w(\max)}$) at this maximum. To appreciate and clarify the structure effects of ions on the conductivities maximum, three different graphs are represented into this manuscript (Figs. 2–4).

In Fig. 2 is plotted the ionic conductivity for four aqueous mixtures of PILs based on the pyrrolidinium cation versus the water weight fraction: [Pyrr][NO₃] (1), [Pyrr][CH₃COO] (2), [Pyrr][HCOO]

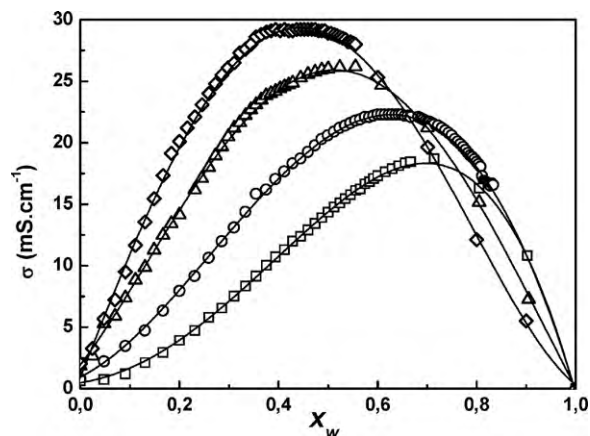


Fig. 3. Ionic conductivity, σ , versus the water weight fraction, w_w , in the aqueous PILs mixtures for formate-based PILs: \blacktriangle , [Pyrr][HCOO] (3); \square , [DIPEA][HCOO] (4); \bullet , [Amil][HCOO] (5); \diamond , [Qui][HCOO] (6); \blacksquare , [Luti][HCOO] (7); \triangle , [Coll][HCOO] (8).

(3), and [Pyrr][C₇H₁₅COO] (11), in order to explore the anion effect on the conductivity for these systems. We can observe that the ionic conductivity presents a maximum at a water weight fraction percentage $w_{w(\max)}$ variable and correlated to the nature of anions from $w_{w(\max)} = 0.42$ for [Pyrr][NO₃] (1) and [Pyrr][HCOO] (3) to $w_{w(\max)} = 0.75$ for [Pyrr][CH₃COO] (2). The increase in the ionic conductivity from the value of the pure PIL to the value at the

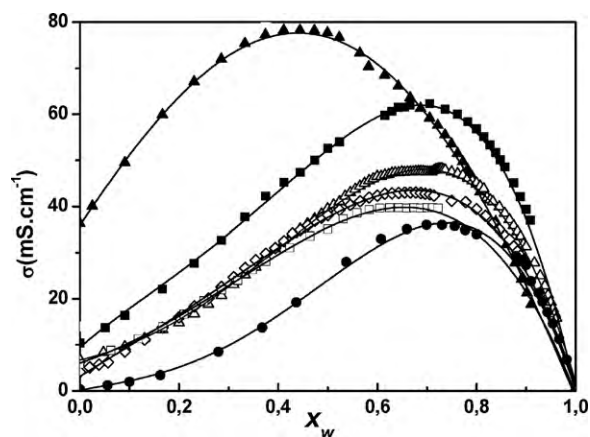


Fig. 4. Ionic conductivity, σ , in the aqueous PILs mixtures versus the water weight fraction, w_w , for alkylcarboxylates-based PILs: \diamond , [Pyrr][C₅H₁₁COO] (9); \triangle , [Pyrr][C₆H₁₃COO] (10); \circ , [Pyrr][C₇H₁₅COO] (11); \square , [Pyrr][C₈H₁₇COO] (12).

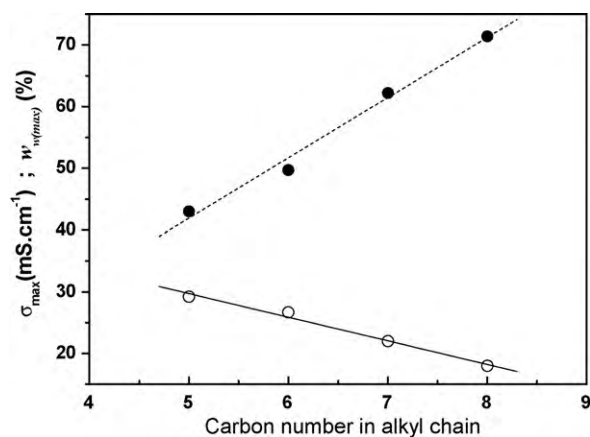


Fig. 5. Dependence of conductivities (σ_{\max} ○) and water weight fraction ($w_{w(\max)}$ ●) as a function of the number of carbon in the alkylcarboxylate chain length for studied pyrrolidinium alkylcarboxylates PILs, [Pyrr][$C_nH_{2n+1}COO$].

maximum varies from 2.2 times for [Pyrr][NO_3] (1) or [Pyrr][HCOO] (3) to 27.8 times for [Pyrr][$C_7H_{15}COO$] (11), respectively.

The “destructuring” effect of water is more important when initial viscosity of PILs is higher. This is the case of [Pyrr][$C_7H_{15}COO$] (11): $\eta = 74.4$ cP, or [Pyrr][CH_3COO] (2): $\eta = 32.2$ cP. The distance between the cation and the anion is not the most important parameter in the “destructuring” effect of water. In fact, for PILs with a long alkyl chain length, the ion-pairs destruction is obtained for higher concentration of water.

In Fig. 3 are presented the ionic conductivity dependences on water weight fraction, w_w , for PILs based on the formate anion: [Pyrr][HCOO] (3); [DIPEA][HCOO] (4); [Amil][HCOO] (5); [Qui][HCOO] (6); [Luti][HCOO] (7); [Coll][HCOO] (8). The curves presented in Fig. 3 are similar to those presented in Fig. 2, in this case (except for [Pyrr][HCOO] (3)), the maximum in the conductivity is shifted toward larger water contents: close to $w_{w(\max)} = 0.70$. For the least conducting PILs, [Amil][HCOO] (5) ($\sigma = 0.36$ mS cm^{-1}), the maximum in conductivity is located at the highest water weight fraction ($\sigma_{\max} = 36.0$ mS cm^{-1} , $w_{w(\max)} = 0.70$). The pyrrolidinium cation, which exhibits more hydrophobic character, is less solvated by water and then more mobile ($\sigma_{\max} = 78.3$ mS cm^{-1} , $w_{w(\max)} = 0.41$).

In Fig. 4, we plot the ionic conductivity for four aqueous mixtures of PILs based on pyrrolidinium alkylcarboxylates PILs, [Pyrr][$C_nH_{2n+1}COO$], with different alkyl chain length on the anion versus the water weight fraction, w_w . We observe, in Fig. 4, that the peaks in the conductivity shift to higher values of water weight fraction, w_w , when the number of carbon on the anion increases, from $w_{w(\max)} = 0.43$ to 0.71 for $n = 5-8$, respectively. At the same time the maximum in conductivity decreases from $\sigma_{\max} = 29.2$ to 18.0 mS cm^{-1} for $n = 5-8$, respectively. The variation of these both factors versus the number of carbon in the anion alkyl chain length is linear as shown in Fig. 5. The van der Waals interactions between hydrophobic carbon chains increase the viscosities and then decrease the conductivities of these PILs. In previous work [26], we show the amphiphilic properties of pyrrolidinium and imidazolium based PILs with long chain alkyl as anion. The micellar properties of these compounds are probably responsible to correlation between conductivity σ , water weight fraction, w_w and the length chain carbon in the anion.

The similarity between the graphs $\sigma = f(w_w)$ reported in Figs. 2–4 indicates that the mechanisms of charge transport must be also the same for all (IL + water) mixtures. When water is added, the density of charge is reduced but the viscosity follows the same trend. At water concentrations above that of the conductivity maximum, the effect of dilution by water is predominant. This shape

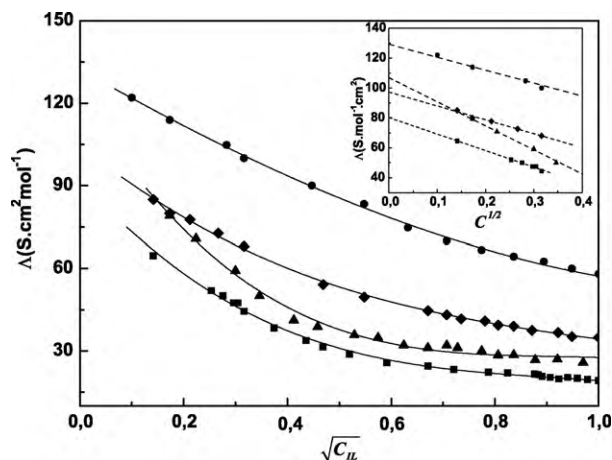


Fig. 6. Debye–Onsager plot of molar conductivity Λ , against $\sqrt{C_{IL}}$ for pyrrolidinium-based PILs in aqueous solutions: ●, [Pyrr][NO_3] (1); ◆, [Pyrr][CH_3COO] (2); ▲, [Pyrr][HCOO] (3); ■, [Pyrr][$C_7H_{15}COO$] (11).

of curve is classically observed for mixtures binary of ionic liquids with molecular solvents [27,28].

There exist two markedly different regions in the conductivity profile of these ionic solutions, corresponding to concentrations below the conductivity maximum, and higher than this value. Although, the effect of coulombic interionic interactions is a monotonic reduction of the mobility of ionic charges in bulk electrolyte solutions over the whole range of concentration, in the first region, the ionic charges can be considered as high-mobility charge carriers so the addition of water to the bulk solution results in an increase of the conductivity. While in the second region, the mobility of the charge carriers is considerably lower because the dilution decreases the interactions between ions. One should reasonably in second physics region of the ionic solution can be understood using conventional transport theory in ionic solutions, thereby treating the medium as a statistical (or diffuse) distribution of ionic charges in a uniform structure less continuum, while in the first region the similitude to a pure IL is progressively less marked. Molénat’s argument for the existence of a maximum in the conductivity/concentration profile must be understood in the electrolyte-like context of the first region [29].

Up to our knowledge, a satisfactory quantitative theoretical explanation of the peak apparition and its position for each salt does not exist, even in electrolyte solution transport theory. Some works try to explain it qualitatively based in the presence of a glassy transition in the aqueous solution at concentrations around the peak [30]. Vila et al. have shown that in the electrical conduction two different mechanisms are present [31]. One of them is the number of ions present to transport charge (which increases with the IL concentration). The other one is related with the mobility of the ions in the solution, which will be lower when the number of ions increases (and so decreases with the concentration). At the peak the addition of both effects is optimal and so the conduction is most effective [31,32].

The molar conductivities, Λ , of the PILs in solution were calculated from the ionic conductivity and the molar concentration, C :

$$\Lambda (\text{S cm}^2 \text{ mol}^{-1}) = 1000 \left(\frac{\sigma}{C} \right) \quad (1)$$

The dependence of the molar conductivity, Λ on the square root of the mole concentration in IL, $\sqrt{C_{IL}}$ (C_{IL} in mol L^{-1}) is illustrated in Figs. 6 and 7, for pyrrolidinium-based and formate-based PILs, respectively. From these graphs, we observed that at high PIL’s concentrations: $C_{IL} > 1.0$ mol L^{-1} , Λ decreases exponentially when

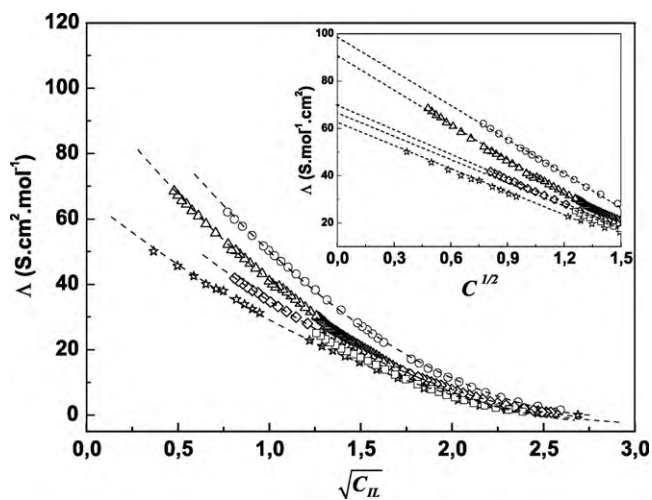


Fig. 7. Kohlrausch plot of molar conductivity, Λ , against $\sqrt{C_{IL}}$ for formate-based PILs in aqueous solutions: \square , [DIPEA][HCOO] (4); \star , [Amil][HCOO] (5); \diamond , [Qui][HCOO] (6); \circ , [Luti][HCOO] (7); Δ , [Coll][HCOO] (8).

C_{IL} increase. This behaviour is characteristic of a weak electrolyte, partially associated in water. This is particularly the case for the pyrrolidinium octanoate (11) which presents a hydrophobic length chain and hence a high tendency to aggregate [26].

To determine the infinite dilution conductances of PILs cations and anions, we plot in the inset of Figs. 6 and 7, the molar conductivity Λ , versus $\sqrt{C_{IL}}$ at low concentrations. The obtained graphs represent a high linearity which is the expected behaviour at infinite dilution [33] according to the Debye–Onsager relation:

$$\Lambda = \Lambda^0 + (a\Lambda^0 + b)\sqrt{C_{IL}} \quad (2)$$

where Λ is the molar conductivity, Λ^0 the infinite dilution molar conductivity, C_{IL} the molar concentration, and a , b the empirical constants. The infinite dilution molar conductivities of the different PILs, Λ^0 , were determined by fitting the experimental data using Eq. (2) and the results are presented in Table 4. In order to evaluate the infinite dilution conductances of the cation or anions of the investigated PILs, the additivity law at infinite dilution was applied a relation as in Eq. (3) was used

$$\Lambda^0 = z_+ \Lambda_+^0 + z_- \Lambda_-^0 \quad (3)$$

Using the infinite dilution conductance of the anions reported in the literature [34].

Infinite dilution conductances data are presented in Table 4. The pyrrolidinium and lutidinium cations have the largest values of $\Lambda_+^0 = 60$ and $45 \text{ S cm}^2 \text{ mol}^{-1}$, respectively, and the amilaminium and quinolinium cations have the smallest values of $\Lambda_+^0 = 10.1$ and $14 \text{ S cm}^2 \text{ mol}^{-1}$, respectively. In the case of pyrrolidinium series with carboxylates anions [Pyrr][$C_nH_{2n+1}COO$], the experimental values $\Lambda^0 = z_+ \Lambda_+^0 + z_- \Lambda_-^0$ are comparable to those obtained in the previous work [26] $\Lambda^0 = 87.2$ ($n=5$), $\Lambda^0 = 85.3$ ($n=6$); $\Lambda^0 = 84.0$ ($n=7$); $\Lambda^0 = 83.0$ ($n=8$), respectively.

The viscosity is an important parameter which can explain the variation of the conductivity of mixtures. For this reason, the conductivities variation of (PIL + water) systems is often linked to their viscosities values.

To correlate viscosity with composition, Seddon et al. [35] have stated that viscosities for ionic liquid mixtures with molecular solvents can generally be described by the exponential expression:

$$\eta = \eta_0 \exp\left[\frac{-x_w}{a}\right] \quad (4)$$

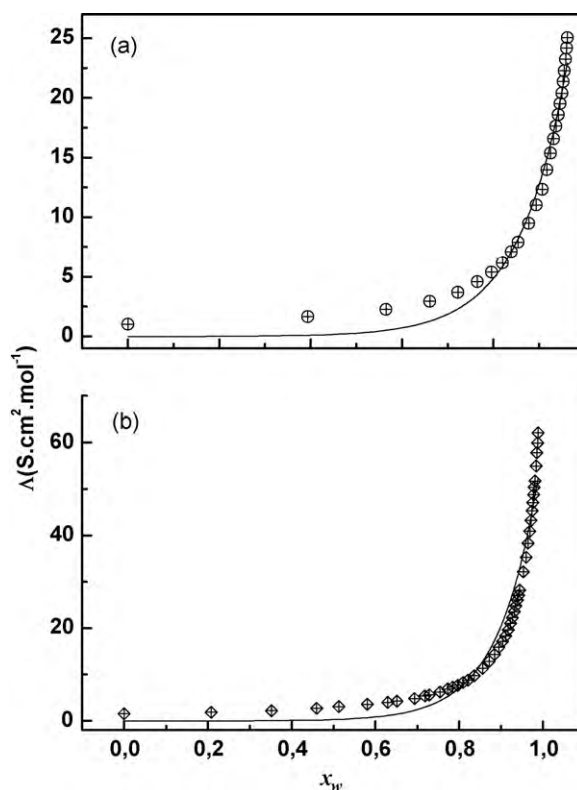


Fig. 8. The molar conductivity for ([DIPEA][HCOO] (4)+water) (a); and ([Luti][HCOO] (7)+water) (b) solutions. The points are experimental data, and the solid lines are the calculated results from Eq. (1), where a is treated purely as an empirical constant.

where η_0 is the dynamical viscosity of the pure IL, x_w the mole fraction of the solvent (water in our case) and a is a fitting parameter, which depends on the types of IL and solvent. The simplest theoretical expression, which relates Λ with the dynamical viscosity, η , is Walden's rule as $\Lambda\eta = k$ [32]. If we suppose that Walden product is valid in all concentration domain and k is not molar fraction, x_w depend, the replace η in Eq. (4) we will relate Λ with the concentration of water in the PIL mixture:

$$\Lambda = \frac{k}{\eta_0} \exp\left(\frac{x_w}{a}\right) = \Lambda_0 \exp\left(\frac{x_w}{a}\right) \quad (5)$$

In order to verify if the present data obey to relationship, the variation of Λ versus the water mole fraction, x_w , have been plotted for four selected samples ([DIPEA][HCOO] (4)+water) in Fig. 8(a), ([Luti][HCOO] (7)+water) in Fig. 8(b), ([Qui][HCOO] (6)+water) in Fig. 9(a) and ([Coll][HCOO] (8)+water) in Fig. 9(b). The continuous lines represent the best fit of Eq. (5) to the presented data. Figs. 8 and 9 show that Eq. (5) correlates correctly the experimental data for (4) and (7) this model is less applicable in the case of (6) and (8).

It can be seen also from Figs. 8 and 9 that for given (PIL + water) solutions, the molar conductivity of the PIL increases with x_w . This observation is easy to understand by considering that the viscosity of the water is much lower than that of the PILs (see Table 2), the addition of water into a PIL can reduce, then, its viscosity significantly [35,36]. Therefore, the mobility of ions or charge carriers is enhanced when the concentration is increased due to the viscosity reduction and finally, the solution becomes more conductive. The conductivity of an electrolyte solution depends on the number and the mobility of the charge carriers [37]. Ion-pairs or larger aggregates exist in both pure PILs and solutions [38], but generally, water, which has a high dielectric constant ($\epsilon = 80$), tends to be completely

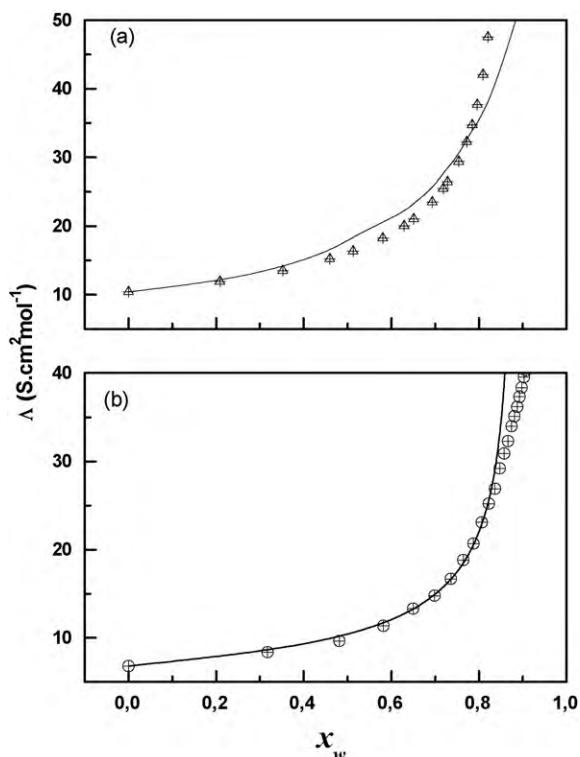


Fig. 9. The molar conductivity for ([Qui][HCOO] (6) + water) (a); and ([Coll][HCOO] (8) + water) (b) solutions. The points are experimental data, and the solid lines are the calculated results from Eq. (1), where a is treated purely as an empirical constant.

solvated with ions of PILs and interacts strongly with them. Therefore, the ability of water to establish H-bond and the electrostatic interactions with ions of PILs, influence the association behaviours of the PILs.

4. Self-diffusion coefficient

Self-diffusion of PILs in water could be considered as the diffusion of a binary univalent electrolyte. Applying the Nernst–Haskell equation [33], the diffusion coefficient of electrolytes is giving by:

$$D_{\text{PIL}}^0 = \frac{RT}{F^2} \frac{|z_+| + |z_-|}{|z_+ z_-|} \frac{\Lambda_+^0 \Lambda_-^0}{\Lambda_+^0 + \Lambda_-^0} \quad (6)$$

where D_{PIL}^0 is the diffusion coefficient of PIL in water at infinite dilution, R the gas constant, T the absolute temperature, F the Faraday's constant, z_+ and z_- are the charge numbers of cation and anion, respectively, Λ_+^0 and Λ_-^0 the infinite dilution conductances of the cation and anion, respectively.

Using infinite dilution molar conductance data of ions reported previously in Table 4, D_{PIL}^0 values of ionic liquids are calculated from Nernst–Haskell equation (Eq. (6)). Results are presented in Fig. 10 and Table 5, with an average error of 5.4%.

In same time, the most common correlation used in order to estimate the diffusion coefficients of organic molecules in a solvent such as the Wilke–Chang equation [39] was used for all studied systems by respecting the following notification: the diffusing component is treated as an organic solute and the diffusion of solute A (PIL) in solvent B (water) is represented by Eq. (7):

$$D_{\text{PIL}/w}^0 = 7.4 \times 10^{-12} \frac{(\phi M_w)^{0.5} T}{\eta_w V_{\text{PIL}}^{0.6}} \quad (7)$$

where $D_{\text{PIL}/w}^0$ is the diffusion coefficient of PIL in water, ϕ the solvent parameter (water: $\phi = 2.26$ [40]), M_w the molecular weight of water,

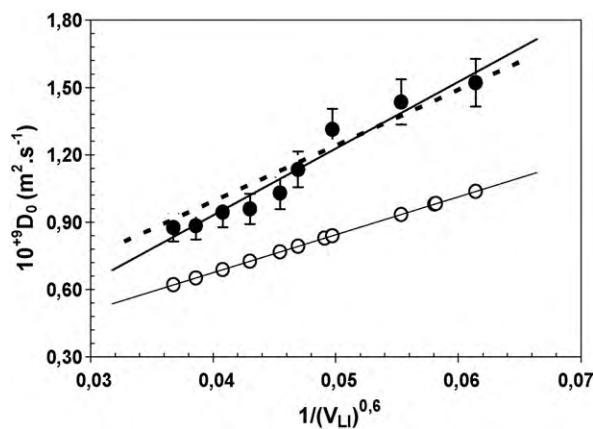


Fig. 10. A Nernst–Haskell (●), Wilke–Chang (○) and modified Wilke–Chang correlation (---) of infinite diffusion coefficients of PILs in water.

T the absolute temperature in K, η_w the viscosity of water in cP, and V_{PIL} is the molar volume of the PIL in $\text{cm}^3 \cdot \text{mol}^{-1}$. These values are available from Table 2. Calculated values of $D_{\text{PIL}/w}^0$ are reported Table 5.

In Fig. 10 is plotted the variation of $D_{\text{PIL}/w}^0$ versus $1/V_A^{0.6}$. As shown in this figure, the diffusion coefficients calculated from Nernst–Haskell equation (Eq. (6)) vary linearly with $1/V_A^{0.6}$, but the Wilke–Chang correlation (Eq. (7)) underestimates these diffusion coefficients. Since the Wilke–Chang equation unsuccessfully represented, a modified Wilke–Chang correlation with a correction factor of k :

$$D_{AB}^0 = k \times \left[7.4 \times 10^{-12} \frac{(\phi M_B)^{0.5} T}{\eta_B V_A^{0.6}} \right] \quad (8)$$

with $k = 1.47$ produced a better correlation of the presented data (Fig. 10) with an average error close to 3.8% (Table 5).

Considering the experimental error involved, the predictions are reasonably accurate. It is interesting to note that the diffusion coefficients of the studied PILs are correlated to the molecular weights as shown in Fig. 11.

The determined self-diffusion coefficients were correlated as a function of viscosity according to the Stokes–Einstein equation [41] to obtain the effective hydrodynamic (or Stokes) radius r_s

$$D^0 = \frac{k_B T}{6\pi\eta_B r_s} \quad (9)$$

where D^0 is the self-diffusion coefficient of PIL at infinite dilution from Nernst–Haskell calculated values, k_B the Boltzmann constant,

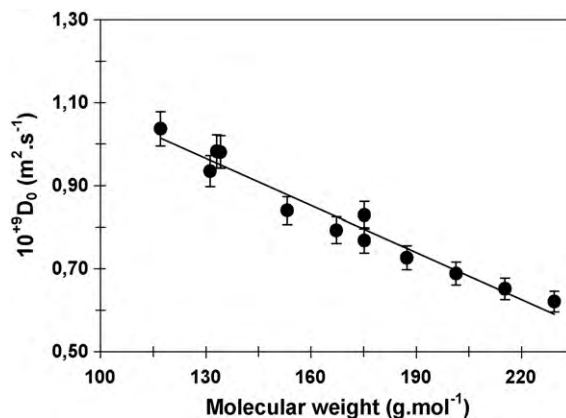


Fig. 11. The variation of infinite self-diffusion coefficients, calculated with the Nernst–Haskell equation, of studied PILs with molecular weights.

Table 5
Self-diffusion coefficients and effective hydrodynamic radius of the studied systems.

PILs	$D^0 \times 10^9$ (m ² s ⁻¹) (Wilke–Chang) equation	$D^0 \times 10^9$ (m ² s ⁻¹) (Nernst–Haskell) equation	$D^0 \times 10^9$ (m ² s ⁻¹) modified (Wilke–Chang) equation	$r_s \times 10^{10}$ (m) (Stokes–Einstein) equation
[Pyr][NO ₃] (1)	0.981	1.760	1.441	2.503
[Pyr][CH ₃ COO] (2)	0.935	1.435	1.374	2.626
[Pyr][HCOO] (3)	1.037	1.521	1.524	2.366
[DIPEA][HCOO] (4)	0.768	1.030	1.129	3.196
[Amil][HCOO] (5)	0.983	0.961	1.444	2.497
[Qui][HCOO] (6)	0.829	0.937	1.219	2.960
[Luti][HCOO] (7)	0.793	1.135	1.165	3.096
[Coll][HCOO] (8)	0.840	1.313	1.235	2.922
[Pyr][C ₅ H ₁₁ COO] (9)	0.726	0.959	1.068	3.378
[Pyr][C ₆ H ₁₃ COO] (10)	0.689	0.944	1.012	3.564
[Pyr][C ₇ H ₁₅ COO] (11)	0.652	0.885	0.958	3.766
[Pyr][C ₈ H ₁₇ COO] (12)	0.621	0.876	0.913	3.953

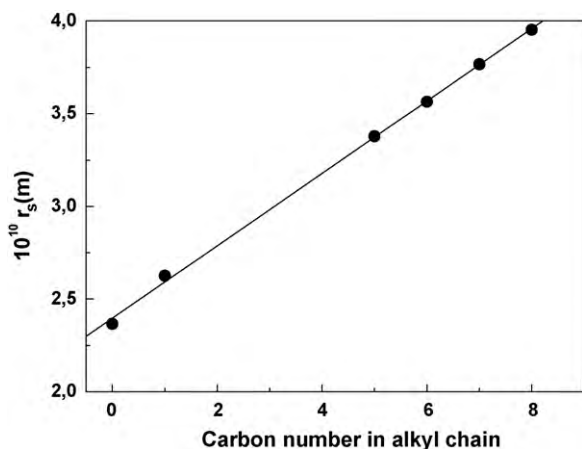
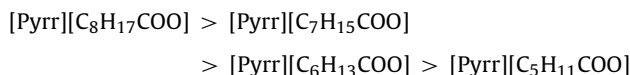


Fig. 12. The variation of the effective hydrodynamic radius of alkylcarboxylates PILs, [Pyr][C_nH_{2n+1}COO], as a function of the anion alkyl chain length, *n*.

and r_s is the effective hydrodynamic (or Stokes) radius. Obtained values of r_s for all PILs are presented in Table 5.

Effective hydrodynamic radius, r_s are from 2.366×10^{-10} to 3.953×10^{-10} m. For comparison for [Emim][BF₄] the r_s value is 3.435×10^{-10} m [42].

For alkylcarboxylates-based PILs, the self-diffusivity decreases as expected with the size of the alkyl chain (both η and r_s increase), that is, following the order:



Heaving alkyl groups usually induce large interionic van der Waals attraction between them, whereas the cation–anion coulombic is reduced owing to steric hindrance. Because the overall result leads to an increased diffusivity, this allows us to assert that the van der Waals attraction between the alkyl chains is a dominant factor determining the self-diffusivity in this system.

Furthermore, as shown in the case of the effective hydrodynamic radius in Fig. 12, the effective hydrodynamic radius, r_s , varies linearly with the anion alkyl chain length on the pyrrolidinium alkylcarboxylates PILs, [Pyr][C_nH_{2n+1}COO].

The following linear relationship can be used in order to correlate the variation of the Stokes radius of pyrrolidinium alkylcarboxylates, [Pyr][C_nH_{2n+1}COO], as a function of the anion alkyl chain length, *n*:

$$r_{S([\text{Pyr}][\text{C}_n\text{H}_{2n+1}\text{COO}])} = r_{S([\text{Pyr}][\text{C}_0\text{H}_1\text{COO}])} + n \times r_{S(-\text{CH}_2-)} \quad (10)$$

where $r_{S(-\text{CH}_2-)}$ is the contribution to the effective hydrodynamic radius of pyrrolidinium alkylcarboxylates of a $-\text{CH}_2-$ group on the alkyl chain and *n* is the number of $-\text{CH}_2-$.

$r_{S([\text{Pyr}][\text{C}_0\text{H}_1\text{COO}])}$ is the effective hydrodynamic radius of the [Pyr][HCOO] (3).

From results reported in Table 5, the best fit was obtained within $r_{S(-\text{CH}_2-)} = (0.195 \pm 0.003) \times 10^{-10}$ m, $r_{S([\text{Pyr}][\text{C}_0\text{H}_1\text{COO}])} = (2.39 \pm 0.01) \times 10^{-10}$ m with an absolute average deviation of 0.7% ($R^2 = 0.9993$). The precision of Eq. (10) gives then the possibility to predict accurately the effective hydrodynamic radius for other pyrrolidinium alkylcarboxylates.

5. Conclusion

The specific conductivities of twelve protic ionic liquids and their mixtures with water in the whole composition range have been determined at 298.15 K and at the atmospheric pressure. The specific conductivities of the (PIL + water) mixtures present a maximum at a water weight fraction, $w_{w(\text{max})}$, which depends strongly of the anion/cation couple considered. The maximum in conductivity, σ_{max} , depends also to the nature of PILs, and the higher reported values are $\sigma_{\text{max}} = 113 \text{ mS cm}^{-1}$ (at $w_{w(\text{max})} = 0.41$) for the ([Pyr][NO₃] + water) solution.

The infinite dilution molar conductivities of the different PILs, are determined by fitting the experimental data to the Kohlrausch equation. The infinite dilution conductances of the cations are then deduced using known values for the anions. These data are used to predict the diffusion coefficient values via the Nernst–Haskell equation. The diffusion coefficients are alternatively calculated by using the original and modified Wilke–Chang equations, but it appears that only the Nernst–Haskell and the modified Wilke–Chang equations are able to give efficiently these values with accuracy. The infinite self-diffusion coefficients of studied PILs are proportional to their molecular weights.

Finally, the effective hydrodynamic radius (Stokes radius) of all studied PILs is determined through the Stokes–Einstein equation. A linear relationship has been then established between the Stokes radius and the number of carbon in the alkyl chain on the carboxylate anion for pyrrolidinium-based PILs. These results can be useful to predict efficiently the radius of other pyrrolidinium alkylcarboxylate.

References

- [1] W. Xu, C.A. Angell, Science 302 (2003) 422–425.
- [2] C.A. Angell, W. Xu, M. Yoshizawa, A. Hayashi, J.-P. Belieres, in: H. Ohno (Ed.), Ionic Liquids: The Front and Future of Material Development, High Technol. Info., Tokyo, 2003, pp. 43–55 (in Japanese, English available from the corresponding author).
- [3] M. Yoshizawa, W. Xu, C.A. Angell, J. Am. Chem. Soc. 125 (2003) 15411–15419.
- [4] T.L. Greaves, A. Weerawardena, C. Fong, I. Krodkiewska, C.J. Drummond, J. Phys. Chem. B 110 (2006) 22479–22487.
- [5] P. Gilli, L. Pretto, V. Bertolasi, G. Gilli, Acc. Chem. Res. 42 (2009) 33–44.
- [6] R. Sheldon, Chem. Commun. (2001) 2399–2407.
- [7] H. Ohno (Ed.), Electrochemical Aspects of Ionic Liquids, Wiley-Interscience, Hoboken, NJ, 2005.

- [8] A.E. Visser, R.P. Swatloski, W.M. Reichert, R.D. Rogers, R. Mayton, S. Sheff, A. Wierzbicki, J.H. Davis Jr., *Chem. Commun.* (2001) 135–136.
- [9] J.L. Anderson, D.W. Armstrong, *Anal. Chem.* 75 (2003) 4851–4858.
- [10] C.M. Gordon, *Appl. Catal. A: Gen.* 222 (2001) 101–117.
- [11] T.L. Greaves, A. Weerawardena, C. Fong, C.J. Drummond, *Langmuir* 23 (2007) 402–404.
- [12] A.J. Walker, N.C. Bruce, *Chem. Commun.* (2004) 2570–2571.
- [13] A. Noda, B. Susan, K. Kudo, S. Mitsushima, K. Hayamizu, M. Watanabe, *J. Phys. Chem. B* 107 (2003) 4024–4033.
- [14] M. Watanabe, T. Mizumura, *Solid State Ionics* 86–88 (1996) 353–356.
- [15] J. Sun, M. Forsyth, D.R. MacFarlane, *J. Phys. Chem. B* 102 (1998) 8858–8864.
- [16] Y. Nakai, K. Ito, H. Ohno, *Solid State Ionics* 113–115 (1998) 199–204.
- [17] A. Noda, M. Watanabe, *Electrochim. Acta* 45 (2000) 1265–1270.
- [18] D.R. MacFarlane, J. Sun, J. Golding, P. Meakin, M. Forsyth, *Electrochim. Acta* 45 (2000) 1271–1278.
- [19] A. Noda, K. Hayamizu, M. Watanabe, *J. Phys. Chem. B* 105 (2001) 4603–4610.
- [20] T. Tsuda, T. Nohira, Y. Nakamori, K. Matsumoto, R. Hagiwara, Y. Ito, *Solid State Ionics* 149 (2002) 295–298.
- [21] T. Nishida, Y. Tashiro, M. Yamamoto, *J. Fluorine Chem.* 120 (2003) 135–141.
- [22] A. Lewandowski, M. Galinski, *J. Phys. Chem. Solids* 65 (2004) 281–286.
- [23] T.M. Pappenfus, W.A. Henderson, B.B. Owens, K.R. Mann, W.H. Smyrl, *J. Electrochem. Soc.* 151 (2004), A209–A215.
- [24] M. Anouti, M. Caillon-Caravanier, C. Le Floch, D. Lemordant, *J. Phys. Chem. B* 112 (2008) 9406–9411.
- [25] M. Anouti, M. Caillon-Caravanier, Y. Dridi, H. Galiano, D. Lemordant, *J. Phys. Chem. B* 112 (2008) 13335–13343.
- [26] M. Anouti, J. Jones, A. Boisset, J. Jacquemin, M. Caillon-Caravanier, D. Lemordant, *J. Colloid Interface Sci.* 340 (2009) 104–111.
- [27] J. Vila, P. Gines, E. Rilo, O. Cabeza, L.M. Varela, *Fluid Phase Equilib.* 247 (2006) 32–39.
- [28] A. Jarosik, S.R. Krajewski, A. Lewandowski, P. Radzinski, *J. Mol. Liq.* 123 (2006) 43–50.
- [29] J. Molenat, *J. Chim. Phys. Physico-Chim. Biol.* 66 (1969) 825–833.
- [30] P. Claes, Y. Loix, J. Glibert, *Electrochim. Acta* 28 (1983) 421–427.
- [31] J. Vila, E. Rilo, L. Segade, O. Cabeza, L.M. Varela, *Phys. Rev. E* 71 (2005) 031201–031208.
- [32] J.O'M. Bockris, A.K.N. Reddy, *Modern Electrochemistry*, vol. 1, Plenum Press, New York, 1998 (Chapter 4).
- [33] R.A. Robinson, R.H. Stokes, *Electrolyte Solutions*, Butterworths, London, 1965.
- [34] P.C. Hiemenz, R. Rajagopalan, *Principles of Colloid and Surface Chemistry*, Marcel Dekker Inc., New York, 1997.
- [35] K.R. Seddon, A. Stark, M.J. Torres, *Pure Appl. Chem.* 72 (2000) 2275–2287.
- [36] J.J. Wang, Y. Tian, Y. Zhao, K. Zhou, *Green Chem.* 5 (2003) 618–622.
- [37] H. Every, A.G. Bishop, M. Forsyth, D.R. MacFarlane, *Electrochim. Acta* 45 (2000) 1279–1284.
- [38] C.S. Consorti, P.A.Z. Suarez, R.F. de Souza, R.A. Burrow, D.H. Farrar, A.J. Lough, W. Loh, L.H.M. da Silva, J. Dupont, *J. Phys. Chem. B* 109 (2005) 4341–4349.
- [39] C.R. Wilke, P. Chang, *AIChE J.* 1 (1955) 264–270.
- [40] B.E. Poling, J.M. Prausnitz, J.P. O'Connell, *The Properties of Gases and Liquids*, fifth ed., McGraw-Hill, New York, 2000.
- [41] K. Hayamizu, Y. Aihara, S. Arai, C.G. Martinez, *J. Phys. Chem. B* 103 (1999) 519–524.
- [42] C.-L. Wong, A.N. Soriano, M.-H. Li, *Fluid Phase Equilib.* 271 (2008) 43–52.